Accepted Manuscript

Depassivation time estimation in reinforced concrete structures exposed to chloride ingress: A probabilistic approach

G. de Vera, C. Antón, M.P. López, M.A. Climent

PII: S0958-9465(16)30891-5

DOI: 10.1016/j.cemconcomp.2016.12.012

Reference: CECO 2758

To appear in: *Cement and Concrete Composites*

Received Date: 21 December 2015

Revised Date: 10 November 2016

Accepted Date: 29 December 2016

Please cite this article as: G. de Vera, C. Antón, M.P. López, M.A. Climent, Depassivation time estimation in reinforced concrete structures exposed to chloride ingress: A probabilistic approach, *Cement and Concrete Composites* (2017), doi: 10.1016/j.cemconcomp.2016.12.012.

Depassivation time estimation in reinforced concrete structures exposed to chloride ingress: a probabilistic approach

G. de Vera[1,*], C. Antón[1], M. P. López[1], M. A. Climent[1]

[a]*Departament d'Enginyeria Civil, Universitat d'Alacant, Ap. 99, 03080 Alacant, Spain*

Abstract

Estimation of depassivation time is a key issue in corrosion prevention. A method to get a probabilistic model from a deterministic one is presented and applied to three simple models: square root of time (SRT), error function (EF) and constant flux (CF) models. Probability distributions of the involved random variables are needed as input parameters. Experimental data have been obtained from a concrete structure exposed to the atmospheric marine environment. These data are analysed to obtain the probability distributions of chloride transport parameters: penetration velocity k (SRT model), diffusion coefficient D (EF and CF models), surface chloride concentration C_S (EF model), and chloride ingress flux J (CF model). These distributions are used to calculate the depassivation time probability distributions according to the three models and the orientation of the samples respect to the sea. This allows to estimate depassivation time for a given depassivation probability.

Keywords: Corrosion, Reinforced concrete, Probability, Chloride

1. Introduction

Port and maritime constructions are infrastructures of high economic and social value. For this reason tools for calculating their service life are of especial interest. In the case of reinforced concrete structures exposed to the marine environment a prime cause of distress is steel corrosion due to chloride ingress [1]. The damage of the structure due to corrosion is produced after the depassivation of steel, which is produced when a high-enough chloride content is reached in the concrete around the steel rebar [2].

Although structural damages only appear after there has been a certain development of the corrosion process, at times the occurrence of steel depassivation has been considered as the event marking the end of service life [2, 3]. This can be considered as a conservative approach, that can be of interest for instance at the design or maintenance phases of the construction of important infrastructures.

The calculations of the end of service life can be carried out through deterministic or probabilistic methods [4]. Deterministic methodologies, which rely on the calculation of the time at which a certain variable reaches a critical value, have been widely used and are even still included in some structural concrete codes [5]. During the last years probabilistic methods for the calculation of service life have gained importance [6–10], since they take into account the uncertainties of the model parameters, thus allowing to introduce the concept of failure probability. The aim of the probabilistic methods is to obtain the probability of an undesirable event (limit state) occurring. In the case of calculations related with the onset of reinforcement corrosion in maritime structures, the conservative limit state would be surpassed when the probability of reaching a critical value for the chloride content at steel depth would be higher than a set value.

Several concrete codes include service life calculation tools [11, 12], which contain their own set of assumptions, for instance regarding the chloride transport model and probability density functions adopted

*Corresponding author
Email address: Guillem.Vera@ua.es (G. de Vera)

Property	Value
Compressive strength (MPa)	25.6
Cement content (kg/m^3)	220
Bulk density (kg/m^3)	2150
Porosity (%)	15.8
Background Cl^- concentration (%)	0.0175

Mean values of at least three samples

Table 1: Properties of the studied concrete

for each one of the considered random variables. They can be fully exploited at the design phase, after setting the duration of the service life and the maximum allowable probability of failure, for calculating appropriate values for some of the design parameters, for instance the minimum reinforcement concrete cover.

Another situation of interest is represented by the surveys of existing structures affected by reinforcement corrosion due to chlorides, for assessing their residual service life [13, 14]. In such cases it is frequent to perform more or less extensive campaigns for obtaining experimental raw data, typically chloride content profiles, and calculated transport parameters representing the performance of the structure. In these cases the abovementioned tools, included in the concrete codes, may represent some rigidity since they use fixed transport models and fixed probability functions for the random variables. The modeler might wish to use some of the available transport models, empirical or physical with different sophistication levels. Furthermore, the experimental sets of data, corresponding to the relevant variables in the models, may fit better to a particular probability function, different from that prescribed in the codes.

The aim of the present work is to present a methodology that allows getting a probabilistic chloride transport model from a deterministic one, thus making possible to calculate the failure probability in relation with the steel depassivation limit state. This is achieved assigning the proper probability distributions to the variables in the deterministic model and computing the corresponding probability distribution of the calculated depassivation time. A method is also proposed for estimating the best choice for the probability density function applicable to any of the random variables. This is accomplished by calculating the minimum value of a newly proposed parameter, α, which represents the difference between the experimental values of the random variables and the values calculated trough any of the available theoretical probability density functions. The difference is integrated over the full domain of the random variable. The proposed procedures provide flexibility to the modeler in choosing the desired empirical transport model, and allow estimating the most adequate probability function for the relevant random variables.

The full methodology has been applied to data obtained from a harbour concrete structure exposed during 30 years to a Mediterranean marine atmosphere. The data were obtained during three field campaigns performed in 1997, 2004 and 2014.

2. Experimental

Concrete cores extracted from the Alacant harbour were studied [15]. Alacant is a Mediterranean city located in the south-east of Spain (38°19'N, 0°29'W). All samples had atmospherical marine exposure conditions and were taken from the Dock 17. This structure was built in 1984 and samples were taken at several locations in 1997 (8 cores), 2004 (6 cores), and 2014 (3 cores). According to the documentation, the structure was fabricated with bulk concrete H-175 [16] and cement used was ordinary Portland cement P-350 [17]. The following tests were performed following standard methods on concrete cores extracted from the studied structure: compressive strength, cement content quantification [18], bulk density, and porosity. Results are shown in Table 1.

Powder samples were obtained from the concrete cores using a profile grinder [19]. This technique allows obtaining powder samples in 2mm intervals. Powder samples were analysed to determine its total chloride

contents. The method used was potentiometric titration [20, 21]. Thus, detailed chloride profiles were obtained. Background chloride concentration (present in concrete before exposure due to raw materials) was determined analysing the innermost part of 11 cores, and the mean value was used. It is shown in Table 1. Bulk density was also determined [22] in order to refer chloride concentrations as $kg\,Cl^{-}/m^{3}$ of concrete instead of mass percentages when necessary. The mean value obtained was used in all calculations involving density.

All calculations were performed using `MATLAB R2013b` software [23]. In particular, integrations were carried out with commands `integral` and `integral3`, which use adaptive methods [24] in order to enhance precission.

3. Probability distributions

Several authors have used statistics to evaluate experimental data regarding chloride ingress and steel depassivation. Normal [25], lognormal [25, 26], beta [12] or gamma distributions [11] have been suggested in the literature for different parameters. Also, some parameters can be studied under the extreme value theory and generalised extreme value distributions (GEV) including Gumbel, Fréchet and Weibull distributions might be applied [27].

Experimental probability distributions have also been used [28]. The experimental probability density function can be estimated from a given set of values $x_i\,(i = 1 \dots N)$ of the random variable X as follows. The domain of the variable is divided in m equally spaced bins of size $\Delta x = (x_{max} - x_{min})/m$, where x_{min} and x_{max} are respectively the minimum and maximum values of the set. Then, the number of values of the set that lay in each bin is counted and the value φ_i of the probability density function in bin i, which is assumed to be constant in the bin, is calculated as:

$$\varphi_i = \frac{n_i}{N\Delta x} \tag{1}$$

where n_i is the number of values that lay in bin i. The smaller the size of bins Δx is, the higher the precision in the probability density function is. Nevertheless, the size of the bin must be large enough to contain a significant number of values n_i. Thus, a precise experimental probability density function can be obtained only if the size of the set of values N is large.

When the precision of the experimental probability distributions is not good enough, the use of theoretical probability distributions is preferable. They can be estimated from the available experimental data. Five kinds of these theoretical probability distributions were used in this paper in order to model the random variables: normal, lognormal, beta, gamma, and Fréchet distributions. All of them depend on two parameters that can be estimated from a given set of values of the random variable. The mean value of the set and the variance of the set are defined respectively as:

$$e = \frac{1}{n}\sum_{i=1}^{n} x_i \quad ; \quad v = \frac{1}{n-1}\sum_{i=1}^{n}(x_i - e)^2 \tag{2}$$

where the set of values of the random variable X is x_i $(i = 1 \dots n)$. Given a theoretical probability distribution of the random variable X, the mean value (or expectation) of the distribution $E(X)$ and the variance of the distribution $Var(X)$ can be estimated as:

$$E(X) \approx e \quad ; \quad Var(X) \approx v \tag{3}$$

The value of the two parameters on which the distribution depends can be solved from equation (3) when appropriate expression for $E(X)$ and $Var(X)$ in terms of the two parameters are substituted here. Normal, lognormal, beta, and gamma probability distributions are summarized in Tables 2 and 3. Information shown in these tables is: the random variable domain, the two parameters on which the distribution depends, the probability density function $\varphi(x)$, the cumulative distribution function $\Phi(x)$, the mean value of the distribution $E(X)$, the variance of the distribution $Var(X)$, and the formulae used to estimate the parameter

	Distribution	
	Normal	Lognormal
Domain	$-\infty < x < +\infty$	$0 \leq x < +\infty$
Parameters	$\mu \in \mathbb{R}, \sigma > 0$	$\mu \in \mathbb{R}, \sigma > 0$
Probability density function $\varphi(x)$	$\frac{1}{\sigma\sqrt{2\pi}} \exp\left(-\frac{(x-\mu)^2}{2\sigma^2}\right)$	$\frac{1}{x\sigma\sqrt{2\pi}} \exp\left(-\frac{(\ln x-\mu)^2}{2\sigma^2}\right)$
Cumulative distribution function $\Phi(x)$	$\frac{1}{2}+\frac{1}{2}\text{erf}\left(\frac{x-\mu}{\sigma\sqrt{2}}\right)$	$\frac{1}{2}+\frac{1}{2}\text{erf}\left(\frac{\ln x-\mu}{\sigma\sqrt{2}}\right)$
$E(X)$	μ	$\exp\left(\mu+\frac{\sigma^2}{2}\right)$
$Var(X)$	σ^2	$\left(\exp\left(\sigma^2\right)-1\right)\exp\left(2\mu+\sigma^2\right)$
Parameters estimation	$\mu = e$	$\mu = \ln\frac{e^2}{\sqrt{v+e^2}}$
	$\sigma = \sqrt{v}$	$\sigma = \sqrt{\ln\left(\frac{v}{e^2}+1\right)}$

Table 2: Normal and lognormal probability distributions

values from a given set of values of the random variable. The mean value of the set e and the variance of the set v are used in these formulae. $\Gamma(x) = \int_0^\infty u^{x-1}\exp(-u)du$ is the gamma function, $\text{erf}(x) = \frac{2}{\sqrt{\pi}}\int_0^x \exp(-u^2)du$ is the error function, $I_{a,b}(x) = \int_0^x u^{a-1}(1-u)^{b-1}du$ $(0 \leq x \leq 1)$ is the incomplete beta function, and $\gamma_a(x) = \int_0^x u^{a-1}\exp(-u)du$ is the lower incomplete gamma function.

Fréchet distribution was developed under the extreme value theory, in which, given a set of random variables with the same distribution, the Fréchet distribution is the one that follows the extreme values (maximum or minimum) of sets of values of these random variables. Fréchet distribution depends on three parameters: $\mu \in \mathbb{R}$, $\sigma, \xi > 0$. The domain of the random variable is $\mu - \frac{\sigma}{\xi} \leq x < +\infty$. The probability density function and the cumulative distribution function are respectively:

$$\varphi(x) = \frac{1}{\sigma}t(x)^{\xi+1}\exp\left(-t(x)\right) \quad ; \quad \Phi(x) = \exp\left(-t(x)\right) \tag{4}$$

where

$$t(x) = \left(1+\left(\frac{x-\mu}{\sigma}\right)\xi\right)^{-1/\xi} \tag{5}$$

The mean value and the variance of the distribution are respectively:

$$E(X) = \begin{cases} \mu + \sigma\dfrac{\Gamma(1-\xi)-1}{\xi} & (\xi < 1) \\ +\infty & (\xi \geq 1) \end{cases} \tag{6}$$

	Distribution	
	Beta	Gamma
Domain	$0 \leq x \leq L$	$0 \leq x < +\infty$
Parameters	$a, b > 0$	$\lambda, k > 0$
Probability density function $\varphi(x)$	$\frac{\Gamma(a+b)}{\Gamma(a)\Gamma(b)L}\left(\frac{x}{L}\right)^{a-1}\left(1-\frac{x}{L}\right)^{b-1}$	$\frac{x^{k-1}}{\Gamma(k)\lambda^k}\exp(-x/\lambda)$
Cumulative distribution function $\Phi(x)$	$\frac{\Gamma(a+b)}{\Gamma(a)\Gamma(b)}I_{a,b}(x/L)$	$\frac{\gamma_k(x/\lambda)}{\Gamma(k)}$
$E(X)$	$\frac{aL}{a+b}$	$k\lambda$
$Var(X)$	$\frac{abL^2}{(a+b+1)(a+b)^2}$	$k\lambda^2$
Parameters estimation	$a = \frac{e^2}{v} - \frac{e^3}{vL} - \frac{e}{L}$ $b = a\left(\frac{L}{e} - 1\right)$	$\lambda = \frac{v}{e}$ $k = \frac{e^2}{v}$

Table 3: Beta and gamma probability distributions

$$Var(X) = \begin{cases} \frac{\sigma^2}{\xi^2}\left(\Gamma(1-2\xi) - \Gamma^2(1-\xi)\right) & \left(\xi < \frac{1}{2}\right) \\ +\infty & \left(\xi \geq \frac{1}{2}\right) \end{cases} \tag{7}$$

We are interested in positive variables. A Fréchet distribution with a positive domain ($0 \leq x < +\infty$) can be obtained if the value $\mu = \sigma/\xi$ is chosen, yielding the two parameter Fréchet distribution whose probability density function and cumulative distribution function are respectively:

$$\varphi(x) = \frac{1}{\sigma}\left(\frac{x\xi}{\sigma}\right)^{-\frac{1+\xi}{\xi}} \exp\left(-\left(\frac{x\xi}{\sigma}\right)^{-\frac{1}{\xi}}\right) \; ; \; \Phi(x) = \exp\left(-\left(\frac{x\xi}{\sigma}\right)^{-1/\xi}\right) \tag{8}$$

Also, the restriction $\xi < \frac{1}{2}$ is imposed because a finite value of $E(X)$ and $Var(X)$ is expected for the studied variables, obtaining:

$$E(X) = \frac{\sigma}{\xi}\Gamma(1-\xi) \quad ; \quad Var(X) = \frac{\sigma^2}{\xi^2}\left(\Gamma(1-2\xi) - \Gamma^2(1-\xi)\right) \tag{9}$$

In order to get the parameter values from these expressions and (3) ξ must be solved from:

$$\frac{\Gamma(1-2\xi)}{\Gamma^2(1-\xi)} = \frac{v}{e^2} + 1 \tag{10}$$

And then σ is calculated as:

$$\sigma = \frac{e\xi}{\Gamma(1-\xi)} \tag{11}$$

4. Probabilistic models

4.1. General formulation

Steel depassivation time t_i in models shown below is written as a function of several random variables whose probability distributions are known. Then, t_i is a random variable whose probability distribution must be determined from the known probability distributions of its variables.

Let X_i $(i = 1 \dots n)$ be n independent random variables with known probability density functions $\varphi_i(x_i)$, and let Y be a random variable calculated from X_i through the expression:

$$Y = f(X_1, X_2, \dots, X_n) \tag{12}$$

Random variable Y is the dependent variable and its probability density function $\psi(y)$ must be found. The probability to find X_i variables simultaneously in the ranges $X_i \in [x_i, x_i + dx_i]$ $(i = 1 \dots n)$ is given by:

$$\varphi_1(x_1)\varphi_2(x_2)\cdots\varphi_n(x_n)dx_1dx_2\cdots dx_n \tag{13}$$

In order to get $\psi(y)$ from this expression, the variable Y must be introduced here. It can be done solving from (12) one of the independent variables (it does not matter which one is chosen). If X_1 is the solved variable:

$$X_1 = g(Y, X_2, \dots, X_n) \tag{14}$$

where g is some function. Then, X_1 becomes the dependent variable and the independent ones are now Y and X_i $(i = 2 \dots n)$. As previously stated, any of the variables can be chosen as the dependent one. Nevertheless, convergence problems can arise when the resulting integrals are evaluated. Thus, in this paper, the dependent variable has been chosen in each case as to avoid convergence problems.

Next, the auxiliary variables A_i are defined as $A_i = X_i$ $(i = 2 \dots n)$ and the variable change from variables $x_1, x_2, \dots, x_n$ to variables $y, a_2, \dots, a_n$ is introduced in (13) yielding:

$$\varphi_1(g(y, a_2, \dots, a_n))\varphi_2(a_2)\cdots\varphi_n(a_n)|J(y, a_2, \dots, a_n)|dyda_2\cdots da_n \tag{15}$$

where J is the Jacobian determinant of the variable change:

$$J(y, a_2, \dots, a_n) = \begin{vmatrix} \partial x_1/\partial y & \partial x_1/\partial a_2 & \cdots & \partial x_1/\partial a_n \\ \partial x_2/\partial y & \partial x_2/\partial a_2 & \cdots & \partial x_2/\partial a_n \\ \vdots & \vdots & \ddots & \vdots \\ \partial x_n/\partial y & \partial x_n/\partial a_2 & \cdots & \partial x_n/\partial a_n \end{vmatrix} \tag{16}$$

Substituting here (14) and the A_i definitions and taking into account that $\partial a_i/\partial a_j = \delta_{ij}$ (δ_{ij} is the Kronecker's delta) and $\partial a_i/\partial y = 0$ (in both cases because Y and $A_i\,(i = 2 \dots n)$ are independent), the evaluation of the determinant yields:

$$J(y, a_2, \dots, a_n) = \frac{\partial g(y, a_2, \dots, a_n)}{\partial y} \tag{17}$$

Then, (15) becomes:

$$\varphi_1(g(y, a_2, \dots, a_n))\varphi_2(a_2)\cdots\varphi_n(a_n)\left|\frac{\partial g(y, a_2, \dots, a_n)}{\partial y}\right| dyda_2\cdots da_n \tag{18}$$

This expression represents the probability to find simultaneously the variable Y in the range $Y \in [y, y+dy]$ and the variables A_i in the ranges $A_i \in [a_i, a_i + da_i]$ $(i = 2 \dots n)$. In order to get the desired probability density function $\psi(y)$, the integration over the auxiliary variables is done, and recalling the A_i definitions, it is finally obtained:

$$\psi(y) = \int\cdots\int \varphi_1(g(y, x_2, \dots, x_n))\left(\prod_{i=2}^{n}\varphi_i(x_i)\right)\left|\frac{\partial g(y, x_2, \dots, x_n)}{\partial y}\right| dx_2\cdots dx_n \tag{19}$$

The integration extends over the full domain of the auxiliary variables.

One, two or four random variables models are used in this paper. The following is obtained particularizing (19) for these cases. The functions f and g for a one random variable model are:

$$y = f(x) \quad ; \quad x = g(y) \tag{20}$$

And (19) becomes:

$$\psi(y) = \varphi(g(y)) \left| \frac{dg(y)}{dy} \right| \tag{21}$$

Where $\varphi(x)$ is the known probability density function of random variable X. No integration is done because no auxiliary variables exist.

The functions f and g for a two random variables model are:

$$y = f(x_1, x_2) \quad ; \quad x_1 = g(y, x_2) \tag{22}$$

And (19) becomes:

$$\psi(y) = \int \varphi_1(g(y, x_2))\varphi_2(x_2) \left| \frac{\partial g(y, x_2)}{\partial y} \right| dx_2 \tag{23}$$

The functions f and g for a four random variables model are:

$$y = f(x_1, x_2, x_3, x_4) \quad ; \quad x_1 = g(y, x_2, x_3, x_4) \tag{24}$$

And (19) becomes:

$$\psi(y) = \iiint \varphi_1(g(y, x_2, x_3, x_4))\varphi_2(x_2)\varphi_3(x_3)\varphi_4(x_4) \left| \frac{\partial g(y, x_2, x_3, x_4)}{\partial y} \right| dx_2 dx_3 dx_4 \tag{25}$$

4.2. Square root of time model

The square root of time (SRT) model is a simple model [5, 29] formulated as:

$$x = k\sqrt{t} \tag{26}$$

Where x (m) is the depth of the critical chloride concentration capable of depassivating the reinforcement, k $(ms^{-1/2})$ is a constant (penetration velocity) and t (s) is exposure time. When the critical chloride concentration reaches the reinforcement ($x = c$, being c the concrete cover depth) the depassivation occurs ($t = t_i$) and corrosion starts. Thus, the depassivation time t_i can be calculated as:

$$t_i = \frac{c^2}{k^2} \tag{27}$$

If k is assumed as a random variable and c as a deterministic one, then a one random variable model is obtained. Its f and g functions are:

$$f(k) = t_i(k) = \frac{c^2}{k^2} \quad ; \quad g(t_i) = k(t_i) = \frac{c}{\sqrt{t_i}} \tag{28}$$

And the probability density function of the depassivation time is calculated with (21) yielding:

$$\psi(t_i) = \frac{1}{2} c t_i^{-3/2} \varphi_k\left(c t_i^{-1/2}\right) \tag{29}$$

where φ_k is the known probability density function of the random variable k. If k and c are assumed as random variables then a two random variables model is obtained. Choosing c as the dependent variable equation (23) gives:

$$\psi(t_i) = \frac{1}{2\sqrt{t_i}} \int k\varphi_c\left(k\sqrt{t_i}\right) \varphi_k(k) dk \tag{30}$$

where φ_c is the known probability density function of random variable c.

4.3. Error function model

The error function (EF) model is a widely used one [30, 31] which is formulated as:

$$C(x,t) = C_S + (C_0 - C_S)\text{erf}\left(\frac{x}{2\sqrt{Dt}}\right) \tag{31}$$

where $C(x,t)$ (kg/m^3) is the chloride concentration at depth x (m) and exposure time t (s), C_S (kg/m^3) is the constant surface chloride concentration, C_0 (kg/m^3) is the background concentration, and D (m^2/s) is the chloride diffusion coefficient. Concentrations can also be expressed as % (referred to concrete or binder mass). When a critical chloride concentration C_{cr} is reached at the concrete cover depth the depassivation occurs $(t = t_i)$ and corrosion starts. I. e., $C(c,t_i) = C_{cr}$, and thus t_i is given by:

$$C_{cr} = C_S + (C_0 - C_S)\text{erf}\left(\frac{c}{2\sqrt{Dt_i}}\right) \tag{32}$$

Depassivation time t_i can be solved from this expression as:

$$t_i = \frac{c^2}{4D\text{inverf}^2\left(\frac{C_S - C_{cr}}{C_S - C_0}\right)} \tag{33}$$

where inverf is the inverse function of the error function. If D and C_S are assumed as random variables and C_{cr}, c, and C_0 as deterministic ones a two random variables model is obtained. Choosing D as the dependent variable the f and g functions are:

$$f(C_S, D) = t_i(C_S, D) = \frac{c^2}{4D\text{inverf}^2\left(\frac{C_S - C_{cr}}{C_S - C_0}\right)} \tag{34}$$

$$g(t_i, C_S) = D(t_i, C_S) = \frac{c^2}{4t_i\text{inverf}^2\left(\frac{C_S - C_{cr}}{C_S - C_0}\right)} \tag{35}$$

And the probability density function of the depassivation time is calculated with (23) yielding:

$$\psi(t_i) = \int \varphi_D(g(t_i, C_S))\varphi_{C_S}(C_S)\left|\frac{\partial g(t_i, C_S)}{\partial t_i}\right| dC_S \tag{36}$$

where φ_{C_S} and φ_D are the known probability density functions of the random variables C_S and D respectively. No depassivation will occurr if $C_S < C_{cr}$ (g is undefined in this case, according to (35)) and then the lower limit of integration variable C_S must be chosen as $C_S = C_{cr}$ and not as $C_S = 0$. If D, C_S, C_{cr}, and c are assumed as random variables and C_0 as a deterministic one a four random variables model is obtained. Choosing C_{cr} as the dependent variable the g function in given by equation (32), and equation (25) yields:

$$\psi(t_i) = \iiint \varphi_{C_{cr}}(g(t_i, D, C_S, c))\varphi_D(D)\varphi_{C_S}(C_S)\varphi_c(c)\left|\frac{\partial g(t_i, D, C_S, c)}{\partial t_i}\right| dDdC_S dc \tag{37}$$

where φ_{C_S} and φ_c are respectively the known probability density functions of the random variables C_S and c.

4.4. Constant flux model

The constant flux (CF) model has been presented in [32] and it assumes a constant chloride ingress flux J $(\frac{kg}{m^2 s})$ and a constant chloride diffusion coefficient D (m^2/s). It is formulated as:

$$C(x,t) = C_0 + 2J\sqrt{\frac{t}{\pi D}}\exp\left(-\frac{x^2}{4Dt}\right) - \frac{Jx}{D}\text{erfc}\left(\frac{x}{2\sqrt{Dt}}\right) \tag{38}$$

where $\mathrm{erfc}(x) = 1 - \mathrm{erf}(x)$ is the complement of the error function. Depassivation occurs ($t = t_i$) when chloride critical concentration C_{cr} is reached at reinforcement depth ($x = c$), i. e. $C(c, t_i) = C_{cr}$, and thus t_i is given by:

$$C_{cr} = C_0 + 2J\sqrt{\frac{t_i}{\pi D}}\exp\left(-\frac{c^2}{4Dt_i}\right) - \frac{Jc}{D}\mathrm{erfc}\left(\frac{c}{2\sqrt{Dt_i}}\right) \tag{39}$$

Depassivation time t_i (f function) cannot be solved analytically from this expression, but can be solved numerically if necessary. If D and J are assumed as random variables and C_{cr}, c, and C_0 as deterministic ones a two random variables model is obtained. Choosing J as the dependent variable the g function is:

$$g(t_i, D) = J(t_i, D) = \frac{C_{cr} - C_0}{2\sqrt{\frac{t_i}{\pi D}}\exp\left(-\frac{c^2}{4Dt_i}\right) - \frac{c}{D}\mathrm{erfc}\left(\frac{c}{2\sqrt{Dt_i}}\right)} \tag{40}$$

And the probability density function of the depassivation time is calculated with equation (23) yielding:

$$\psi(t_i) = \int \varphi_J(g(t_i, D))\varphi_D(D)\left|\frac{\partial g(t_i, D)}{\partial t_i}\right| dD \tag{41}$$

where φ_J and φ_D are the known probability density functions of the random variables J and D respectively. If D, J, C_{cr}, and c are assumed as random variables and C_0 as a deterministic one a four random variables model is obtained. Choosing C_{cr} as the dependent variable the g function is given by equation (39), and equation (25) yields:

$$\psi(t_i) = \iiint \varphi_{C_{cr}}(g(t_i, D, J, c))\varphi_D(D)\varphi_J(J)\varphi_c(c)\left|\frac{\partial g(t_i, D, J, c)}{\partial t_i}\right| dDdJdc \tag{42}$$

where φ_J and φ_c are respectively the known probability density functions of the random variables J and c.

5. Results and discussion

5.1. Probability distributions

Two examples of representative experimental chloride concentration profiles are shown in Figure 1. They correspond to cores extracted at the same place but at different ages. One was extracted in 1997 (13 years age) and the other was extracted in 2014 (30 years age). In most cases, as the ones shown in the Figure, the presence of a peak can be observed. This is probably due to convective transport processes between surface and the maximum [33].

Each experimental profile has been fitted to the three presented transport models (SRT, EF, and CF) in order to get the values of the transport parameters on which they depend (k, D (EF and CF models), C_S, and J). In this way a set of values for each transport parameter is obtained and they can be treated as random variables.

A representative value [11, 12, 34] for the critical chloride concentration equal to 0.05% referred to concrete mass has been considered for SRT model. The location x (from the maximum inwards [35]) in the profile where this concentration is located is searched and then the k value is calculated as $k = x/\sqrt{t}$, where t is the age of the profile. For EF and CF models, the experimental profiles have been fitted to equations (31) and (38) respectively, obtaining the corresponding transport parameters. Only the points from the maximum inwards have been used for the fitting, which is a common practice in profile treatment [35]. One of the profiles did not met the minimum requirements to be fitted [36] and was discarded. Background chloride concentration C_0 used is shown in Table 1.

Concrete cores have been divided in two groups according to their orientation: exposed to sea and protected from sea, and the mean value e and the standard deviation (square root of variance) $s = \sqrt{v}$ for the obtained set of values of each transport parameter are shown in Table 4. Number of samples is $n = 8$ for each group. A t-Student test shows that mean values for both orientation groups are significantly different ($p = 0.05$) for the random variables k, C_S, and J. And they are not significantly different for variable D (EF

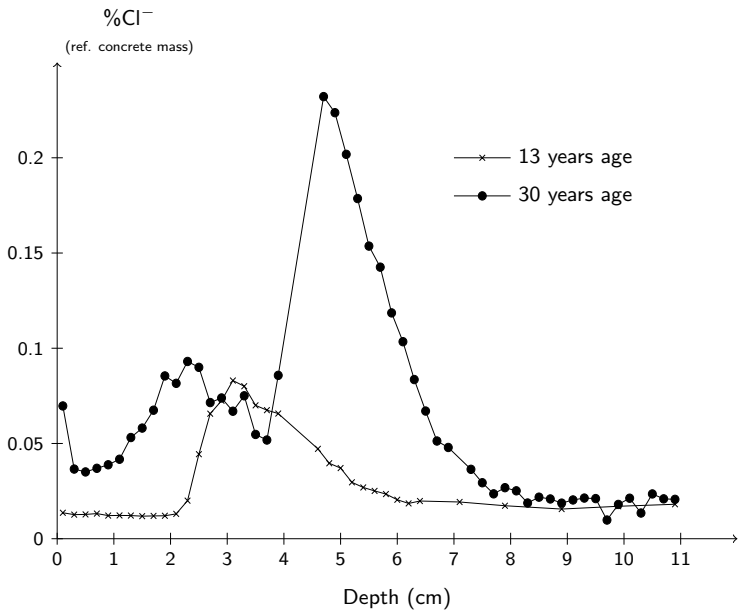

Figure 1: Experimental chloride concentration profiles from cores extracted at the same place in 1997 (cross, 13 years age) and in 2014 (circle, 30 years age)

and CF models). Surface concentration C_S and chloride ingress flux J are related with exposure conditions and thus a difference between both groups is expected. It is worth noting also that the mean values of these variables are higher for the group oriented towards the sea, for which a higher chloride supply is expected. On the other hand, diffusion coefficient D is more related with concrete properties. As the concrete is the same in both orientations a difference is not expected. This is confirmed with the t-Student test. The SRT model uses only one parameter and thus k is influenced by both exposure conditions and concrete properties. Then, a difference between both groups is expected and observed. Nevertheless, the difference is lower for k (which includes both effects) than for C_S and J (which are more influenced by exposure conditions). Exposed to protected ratio of mean values is about 1.5 for k, about 1.8 for C_S, and about 2.5 for J. Some authors [37–40] have found a time dependence of D and C_S that has been attributed to cement maturation [37]. In this paper, no time dependence is observed on the transport parameters when a t-Student test is performed on data from profiles of different ages. This fact can be explained because the first cores were extracted when the structure was at least 13 years old. An ordinary Portland cement is well maturated at this age and a variation in transport parameters is not expected.

The experimental probability density functions for the random variables have been calculated as described previously. A small number of bins ($m = 3$) has been considered due to the small number of samples available (8 samples per group), resulting in a low precision for the experimental probability density functions. Experimental probability density functions are shown in Figures 2, 3, and 4 (histograms) for models SRT, EF and CF respectively.

As the precision of the experimental probability distributions is not good, it is convenient to use theoretical ones. Data in Table 4 have been used to fit each random variable to the five probability distributions as previously explained. Parameter ξ of Fréchet distribution has been solved tabulating $y = \Gamma(1-2\xi)/\Gamma^2(1-\xi)$ versus ξ ($0 < \xi < \frac{1}{2}$) and interpolating the ξ value which provides $y = \frac{v}{e^2} + 1$. Results are shown in Table 5. Only data for the best fitted distributions (see below) for each parameter and orientation is shown.

In order to determine which of the five theoretical distributions is the best choice for each random

Model	Random variable	Exposure to sea	Mean value e	Standard deviation s
SRT	k	exposed	2.0888	0.3754
		protected	1.4694	0.3494
EF	D	exposed	1.6091	0.8469
		protected	0.9882	0.4711
	C_S	exposed	1.8976	0.7124
		protected	1.0245	0.7890
CF	D	exposed	2.1534	1.2058
		protected	1.2246	0.6200
	J	exposed	2.5169	0.9853
		protected	1.0108	0.6462

k in $cm/year^{1/2}$, D (EF and CF models) in $10^{-12}m^2/s$, C_S in %, J in $10^{-9}kg/(m^2s)$

Table 4: Mean value and standard deviation for the set of values of each transport parameter

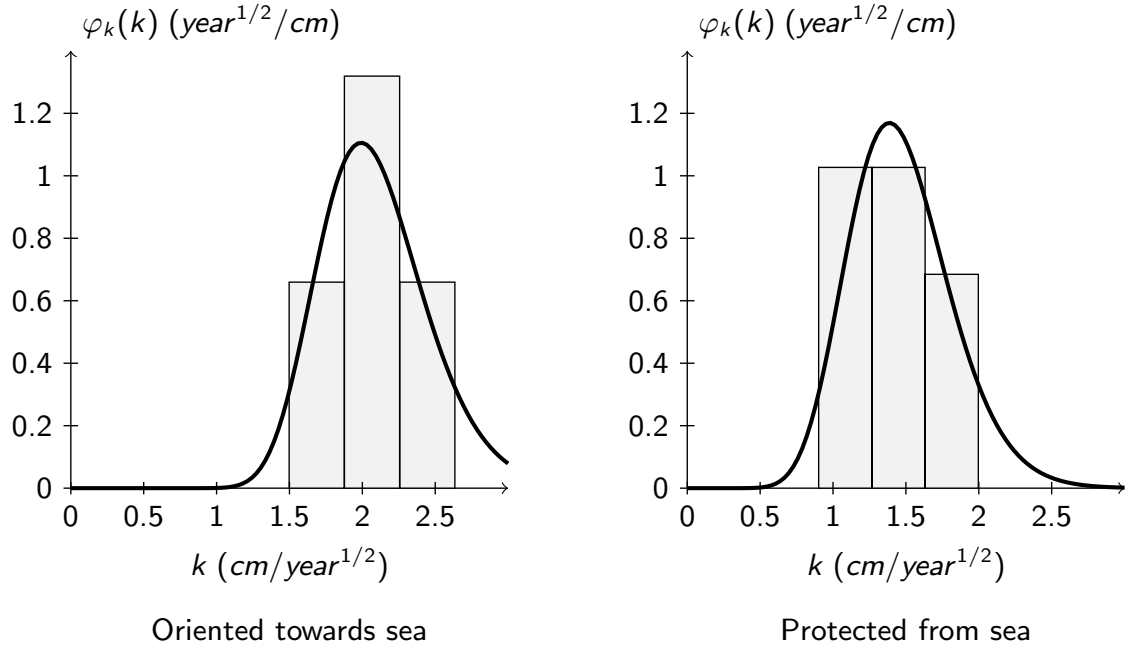

Figure 2: SRT model. Experimental (histogram) and fitted (line) probability density functions of random variable k. Samples orientation: towards sea (left) and protected from sea (right). Fitted distributions are respectively lognormal and gamma

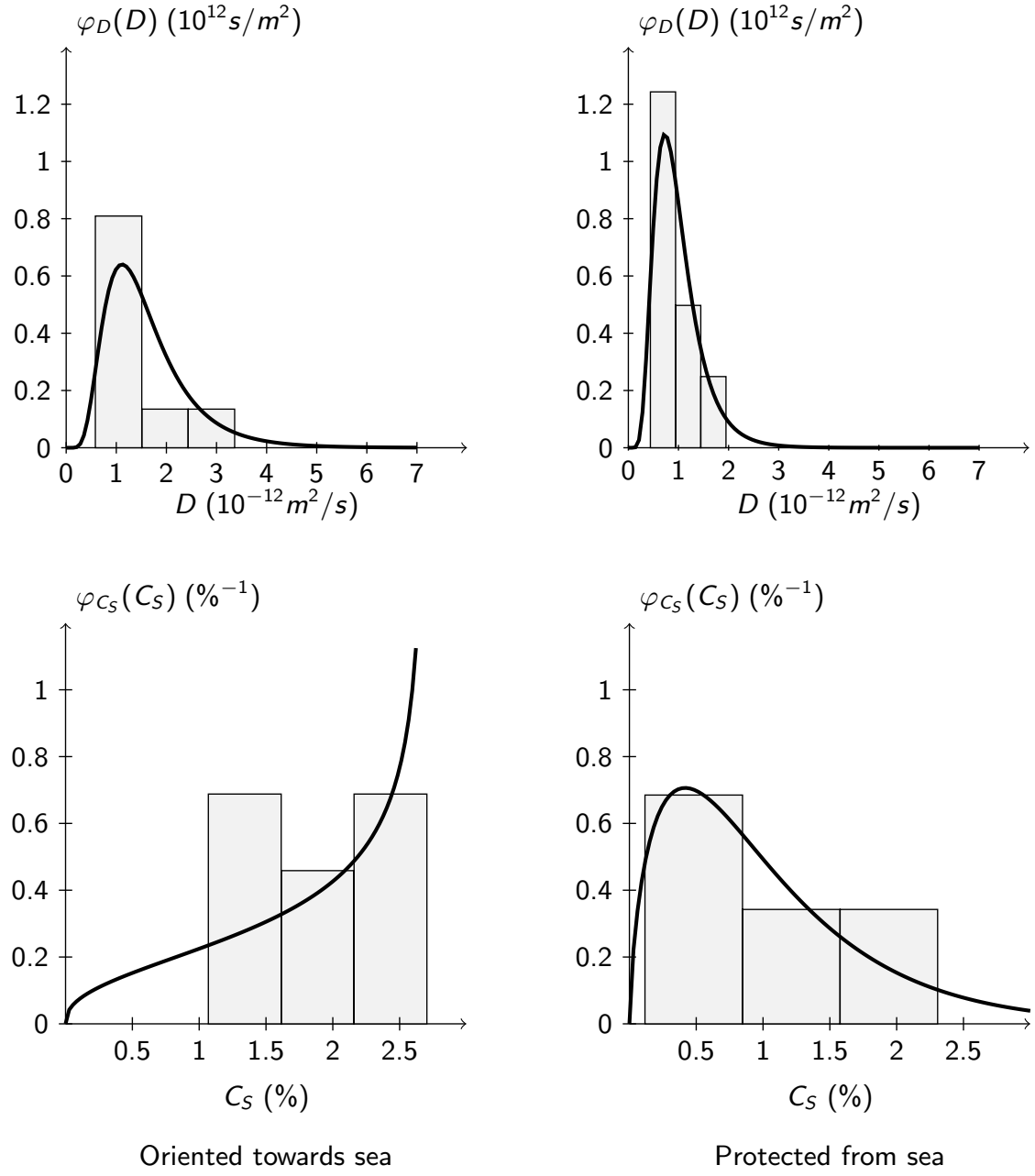

Figure 3: EF model. Experimental (histogram) and fitted (line) probability density functions. Random variable D for the group oriented towards sea (top-left) and for the group protected from sea (top-right), and random variable C_S for the group oriented towards sea (bottom-left) and for the group protected from sea (bottom-right). Fitted distributions are respectively lognormal, lognormal, beta, and gamma

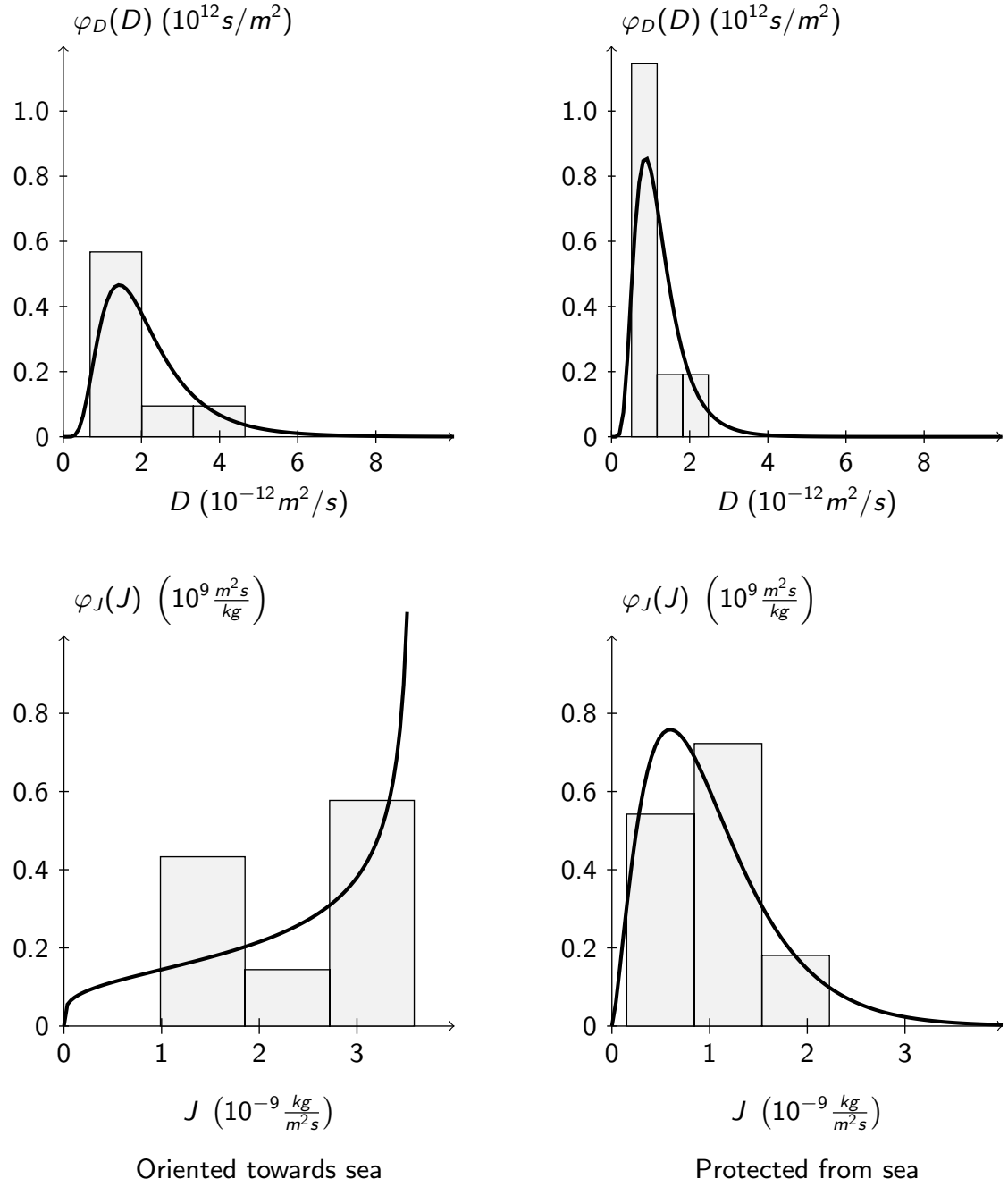

Figure 4: CF model. Experimental (histogram) and fitted (line) probability density functions. Random variable D for the group oriented towards sea (top-left) and for the group protected from sea (top-right), and random variable J for the group oriented towards sea (bottom-left) and for the group protected from sea (bottom-right). Fitted distributions are respectively lognormal, lognormal, beta, and gamma

Model	Variable[1]	Exposure	Distribution[2]	Parameters[3]	
SRT	k	Exposed	LN	$\mu = 0.7207$	$\sigma = 0.1783$
		Protected	G	$\lambda = 0.0831$	$k = 17.6866$
EF	D	Exposed	LN	$\mu = -27.2776$	$\sigma = 0.4945$
		Protected	LN	$\mu = -27.7453$	$\sigma = 0.4525$
	C_S	Exposed	B ($L = 2.7041$)	$a = 1.4146$	$b = 0.6012$
		Protected	G	$\lambda = 0.6076$	$k = 1.6861$
CF	D	Exposed	LN	$\mu = -27.0003$	$\sigma = 0.5222$
		Protected	LN	$\mu = -27.5425$	$\sigma = 0.4777$
	J	Exposed	B ($L = 3.5861 \cdot 10^{-9}$)	$a = 1.2437$	$b = 0.5283$
		Protected	G	$\lambda = 4.1317 \cdot 10^{-10}$	$k = 2.4463$

[1] k in $cm/year^{1/2}$, D (EF and CF models) in m^2/s, C_S in %, J in $\frac{kg}{m^2 s}$

[2] N = normal, LN = lognormal, B = beta, G = gamma, F = Fréchet

[3] L, normal parameters, λ, and σ (Fréchet) have the same units as its variable
Lognormal parameters, a, b, k, and ξ are adimensional

Table 5: Fitted probability distributions for the random variables. Only the best fit for each parameter and orientation is shown

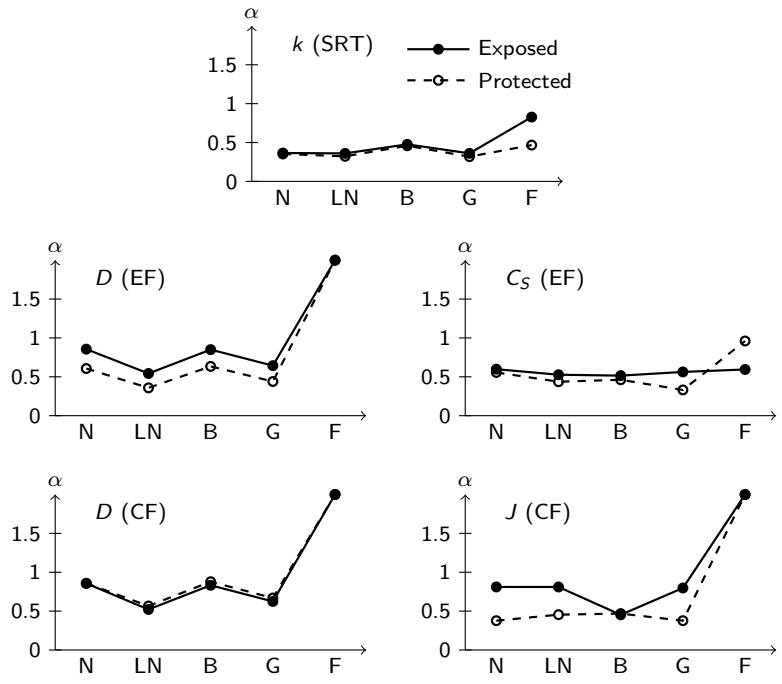

Figure 5: α values for the fitted distributions. SRT model (top), EF model (middle), and CF model (bottom). Distributions are: N = normal, LN = lognormal, B = beta, G = gamma, and F = Fréchet

variable, the following has been calculated:

$$\alpha = \int |\varphi_{theor}(x) - \varphi_{exp}(x)| dx \tag{43}$$

where $\varphi_{exp}(x)$ is the experimental probability density function of random variable X and $\varphi_{theor}(x)$ is the fitted theoretical one. Integration extends over the full domain of the variable and it can be solved analytically if the domain is divided in appropriate intervals in which the integrand sign is constant. Results are shown in Figure 5. The value of α represents how much the theoretical distribution differs from the experimental one. Thus, the lower the α value is, the better the fit is. According to data from Figure 5, the best fitted distributions for the group oriented towards sea are lognormal for k and D (EF and CF models), and beta for C_S and J. And the best fitted distributions for the group protected from sea are lognormal for D (EF and CF models), and gamma for k and C_S. Lower α value for J is obtained for normal distribution, but this distribution is not acceptable because it yields significant probability outside the domain of the variable (negative values). The next lower α value is obtained with a gamma distribution, so this distribution is used for J in the protected group. The best fitted theoretical distributions are also shown in Figures 2, 3, and 4 (lines), where they are compared with their corresponding experimental distributions (histograms).

5.2. Steel depassivation times

The depassivation time probability density functions $\psi(t_i)$ of the two groups of samples have been calculated using the three presented models. The fitted probability density functions of the random variables k, D (EF and CF models), C_S, and J have been used for this purpose. Also, the concrete cover depth c and the critical chloride concentration C_{cr} are needed. Experimental values of these variables are not available for the studied structure and the representative values $c = 7cm$ [5] and $C_{cr} = 0.05\%$ [11, 12, 34] have been chosen. For each group and for each model two cases have been calculated. In one case c and C_{cr} have been considered as deterministic values and in the other case they have been considered as random variables. k, D (EF and CF models), C_S, and J have been considered random in all cases. A normal distribution with $\mu = 7cm$ and $\sigma = 0.5cm$ has been considered for c [5, 9], and a lognormal distribution with $\mu = -3.0699$ and $\sigma = 0.3853$ (that correspond to a mean value of 0.05% and a standard deviation of 0.02%) has been considered for C_{cr} [11, 12, 34]. As previously stated, integration extends over the full domain of random variables. When lognormal and gamma distributions are used, this domain extends to infinity and the upper integration limit must be bounded in order to evaluate the integral. In these cases the upper limit has been bounded to achieve a 99.99% probability, i. e., the upper limit have been set to $icdf(0.9999)$, where $icdf$ is the inverse of the cumulative distribution function. Due to convergence problems during integration, depassivation time probability densitiy function could not be obtained for the following cases: exposed group using EF model with 4 random variables, and exposed group using CF model with 4 random variables. The resulting probability density functions are then integrated (trapezoidal rule with 1000 points in 100 years range) in order to obtain their corresponding cumulative distribution functions, which provide depassivation probability as a function of exposure time:

$$\Phi(t_i) = \int_0^{t_i} \psi(t) dt \tag{44}$$

The obtained cumulative distribution functions are shown in Figures 6, 7, and 8 for the SRT, EF, and CF models respectively. The deterministic depassivation time $t_{i,det}$ is also shown in these figures. It has been calculated using the mean values of the random variables and equations (27), (33), and (39) for SRT, EF, and CF models respectively.

A different behaviour between exposed samples (lines and symbols) and protected samples (lines) can be observed in figures 6, 7, and 8. The increase of depassivation probability with time is slower for samples protected from sea, as expected. The difference between both groups of samples is higher for the SRT model and it is lower for the EF model. If the cases where c and C_{cr} have been considered as deterministic (solid line), are compared with the cases where they have been considered random (dotted line), a small difference in behaviour is observed between both cases. In this case, the uncertainty due to c and C_{cr} is less important

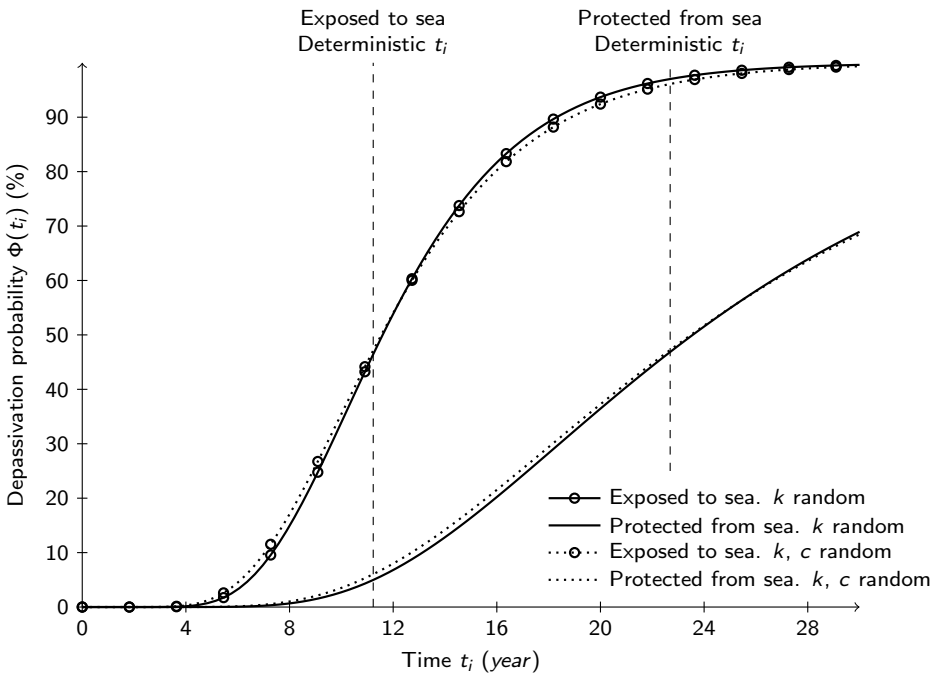

Figure 6: SRT model. Calculated depassivation time cumulative distribution functions

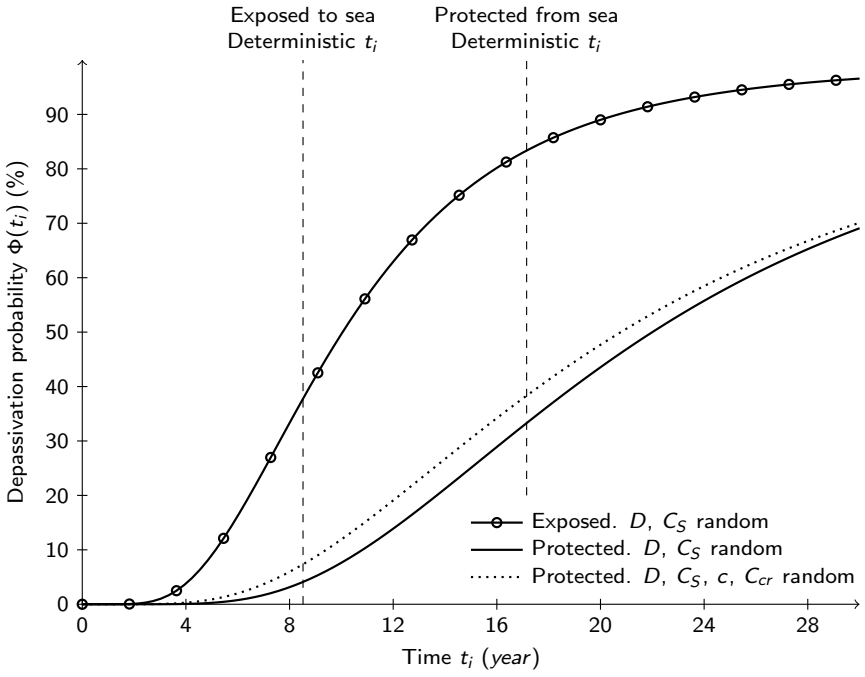

Figure 7: EF model. Calculated depassivation time cumulative distribution functions

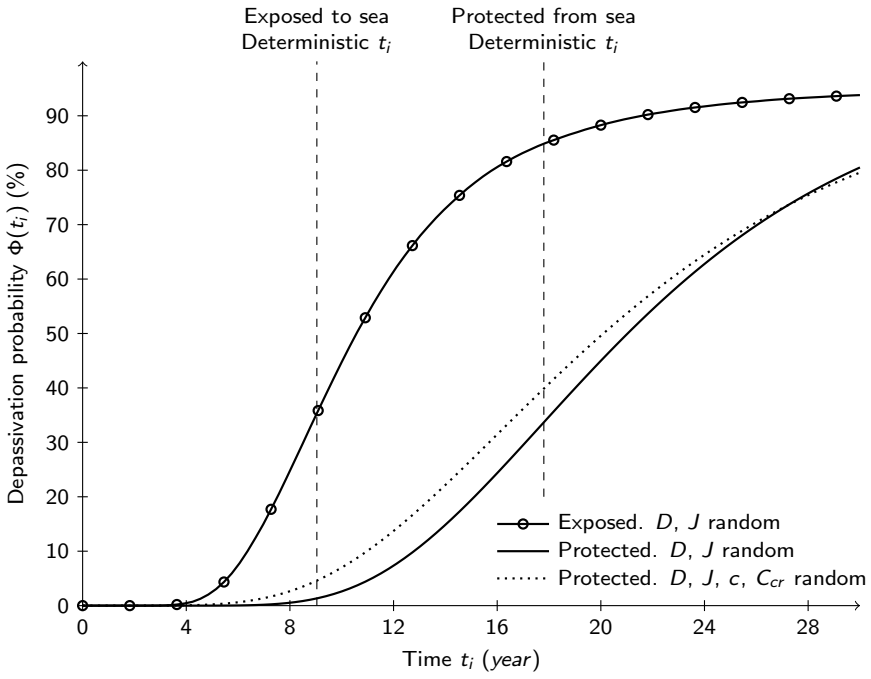

Figure 8: CF model. Calculated depassivation time cumulative distribution functions

than the one due to k, D, and J. Although this difference is small, it can be observed that depassivation probability increase is faster (specially at short times) when the number of random variables is higher, due to the increase of uncertainty when more random variables are considered.

Depassivation probability at deterministic times $\Phi(t_{i,det})$ can be interpolated in Figures 6, 7, and 8. They are shown in Table 6 and they are approximately in the range 30% to 40% for EF and CF models and in the range 45% to 50% for SRT model. These are high values. This means that if the deterministic depassivation time is considered for maintenance or repair then there is a high probability of corrosion even before reparation takes place. This is the reason why some codes [12, 41] recommend taking into account probability and performing reparations at a time when corrosion probability is still low. Values of 7% [41] and 10% have been proposed [12]. The depassivation time for a given probability can be interpolated in figures 6, 7, and 8. Table 6 shows depassivation times for 10% depassivation probability $t_{10\%}$. As expected, $t_{10\%}$ is higher for samples protected from sea. Nevertheless, the difference in $t_{10\%}$ between exposed and protected samples is lower than the difference in the deterministic depassivation times. If the number of random variables is considered, a slightly lower value of $t_{10\%}$ is obtained when the number of random variables is higher, due to the increase of uncertainty when more random variables are considered.

6. Conclusions

A versatile methodology to estimate the probabilistic depassivation time for a reinforced concrete marine structure is presented. This methodology allows:

- To choose the model and the limit state function that better represents the event that marks the end of service life.
- To select the best probabilistic function for the parameters involved in the model, on the basis of experimental data obtained by testing concrete specimens collected from the structure.

Model	Exposure to sea	$t_{i,det}$ $(year)$	Random variables	$t_{10\%}$ $(year)$	$\Phi(t_{i,det})$ (%)
SRT	Exposed	11.23	k	7.34	46.4
			k, c	7.04	47.1
	Protected	22.69	k	13.13	46.9
			k, c	12.70	47.2
EF	Exposed	8.52	D, C_S	5.15	37.8
			D, C_S, c, C_{cr}	—	—
	Protected	17.15	D, C_S	10.82	33.3
			D, C_S, c, C_{cr}	9.41	38.3
CF	Exposed	9.04	D, J	6.36	35.3
			D, J, c, C_{cr}	—	—
	Protected	17.80	D, J	12.79	33.7
			D, J, c, C_{cr}	10.97	39.9

Table 6: Calculated depassivation times

Three diffusion models have been employed as a limit state function. That is, the square root of time model, the error function model and the constant flux model.

The abovementioned methodology has been applied to data obtained from a structure exposed during 30 years to an atmospheric marine environment. The probability density functions of the random variables were obtained from the fitting of the experimental data collected in three different campaigns, 1997, 2004 and 2014. Data were fitted to five theoretical distributions: normal, lognormal, beta, gamma, and Fréchet. In order to determine which of the theoretical distributions better fits the experimental data, a criteria represented by the α parameter has been proposed in this work.

The development of a t-Student test shows the need to divide specimen data into two different groups (exposed to sea and protected from sea) since the mean values of the transport parameters are significantly different. Also, t-Student test shows no time dependence of transport parameters in this study.

For a given failure probability of 10% (recommended by most concrete codes) probabilistic depassivation times obtained are lower than the deterministic ones for the three transport models analyzed in this work.

Acknowledgements

This work has been financially supported by the Ministerio de Economía y Competitividad of Spain and Fondo Europeo de Desarrollo Regional (FEDER) through project BIA2010-20548. We are also indebted to the Autoridad Portuaria de Alicante/Alacant (Alicante/Alacant Harbour Authority) for allowing the sampling campaigns performed at Dock number 17. M. P. López is grateful for a fellowship of the "Formación Personal Investigador (FPI)" programme (reference BES-2011-046401).

References

[1] V. M. Malhotra, editor. *Proceedings of the 3rd CANMET/ACI International Conference. SP-163 on Performance of concrete in marine environment.*, Farmington Hills, Michigan, USA, 1996. ACI.

[2] L. Bertolini, B. Elsener, P. Pedeferri, and R. Polder. *Corrosion of Steel in Concrete. Prevention, Diagnosis, Repair*, chapter Design for durability, pages 165–192. Wiley-VCH, Weinheim, Germany, 2004.

[3] A. Costa and J. Appleton. Chloride penetration into concrete in marine environment. —Part II: Prediction of long term chloride penetration. *Mater and Struct*, 32:354–359, 1999.

[4] P. B. Bamforth. *Enhancing Reinforced Concrete Durability. Guidance on Selecting Measures for Minimising the Risk of Corrosion of Reinforcement in Concrete. Technical Report No. 61*, chapter Service-life design and probabilistic modeling, pages 147–152. The Concrete Society, Surrey, UK, 2004.

[5] Ministerio de Fomento. *Instrucción de Hormigón Estructural EHE-08 (Structural Concrete Code EHE-08)*. Madrid, Spain, 2008. (In Spanish).

[6] A. Vrouwenvelder and P. Schießl. Durability aspects of probabilistic ultimate limit state design. *Heron*, 44(1):19–30, 1999.

[7] T. J. Kirkpatrick, R. E. Weyers, C. M. Anderson-Cook, and M. M. Sprinkel. Probabilistic model for the chloride-induced corrosion service life of bridge decks. *Cement and Concrete Research*, 32:1943–1960, 2002.

[8] D. V. Val and P. A. Trapper. Probabilistic evaluation of initiation time of chloride-induced corrosion. *Reliability Engineering and System Safety*, 93:364–372, 2008.

[9] L. Bertolini. Performance-based service life design of reinforced concrete structures exposed to chloride environments. In L. Dezi, G. Moriconi, and R. Realfonzo, editors, *Proc. of the 2nd Workshop on The New Boundaries of Structural Concrete*, pages 17–30, Ancona, Italy, 2011. ACI.

[10] P. C. Ryan and A. J. O'Connor. Probabilistic analysis of the time to chloride induced corrosion for different self-compacting concretes. *Construction and Building Materials*, 47:1106–1116, 2013.

[11] Brite EuRam III. Duracrete r17. duracrete Final technical report. General guidelines for durability design and redesign. Document be95-1347/r17, The European Union - Brite EuRam III, DuraCrete - Probabilistic performance based durability design of concrete structures, CUR, Gouda, The Netherlands, 2000.

[12] Model code for service life design of concrete structures. Fib Bulletin no. 34, Fédération Internationale du Béton (fib), Lausanne, Switzerland, 2006.

[13] I. Stipanovic, D. Bjegovic, and D. Mikulic. Evaluation of service life design models on concrete exposed to marine environment. *Materials and Structures*, 43:1397–1412, 2010.

[14] S. M. S. Samarakoon and J. Sælensminde. Condition assessment of reinforced concrete structures subject to chloride ingress: A case study of updating the model prediction considering inspection data. *Cement and Concrete Composites*, 60:92–98, 2015.

[15] E. Viqueira. *Contaminación por cloruros del hormigón debida a la interacción con los productos de combustión del PVC y a la exposición a una atmósfera marina (Concrete contamination by chlorides due to interaction with PVC combustion products and due to marine atmospherical exposure)*. PhD thesis, Universitat d'Alacant, Alacant, Spain, 2009. (In Spanish).

[16] MOPU. *Real Decreto 2252/1982: Instrucción para el proyecto y ejecución de obras de hormigón en masa o armado (EH-82)*. Boletín Oficial del Estado (BOE), Madrid, Spain, 24 july 1982. Ministerio de Obras Públicas y Urbanismo (In Spanish).

[17] MOPU. *Real Decreto 1964/1975: Pliego de prescripciones técnicas generales para la Recepción de Cemento (RC-75)*. Boletín Oficial del Estado (BOE), Madrid, Spain, 23 may 1975. Ministerio de Obras Públicas y Urbanismo (In Spanish).

[18] S. Chinchón, J. García, M. López Atalaya, A. Linares, and R. Vera. Cement paste colouring in concretes. *Cem Concr Res*, 34:1987–1991, 2004.

[19] Ø. Vennesland, M. A. Climent, and C. Andrade. Recommendation of RILEM TC 178-TMC: Testing and modeling chloride penetration in concrete. Methods for obtaining dust samples by means of grinding concrete in order to determine the chloride concentration profile. *Mater and Struct*, 46:337–344, 2013.

[20] M. A. Climent, E. Viqueira, G. de Vera, and M. M. López Atalaya. Analysis of acid-soluble chloride in cement, mortar and concrete by potentiometric titration without filtration steps. *Cem Concr Res*, 29:893–898, 1999.

[21] M. A. Climent, G. de Vera, E. Viqueira, and M. M. López. Generalization of the possibility of eliminating the filtration step in the determination of acid-soluble chloride content in cement and concrete by potentiometric titration. *Cem Concr Res*, 34(12):2291–2295, 2004.

[22] ASTM C642-90. *Standard Test Method for Specific Gravity, Absorption, and Voids in Hardened Concrete*.

[23] *MATLAB*. The MathWorks, Inc., 3 Apple Hill Dr., Natick, USA. URL http://www.mathworks.com/help/matlab/index.html.

[24] L.F. Shampine. Vectorized adaptive quadrature in MATLAB®. *Journal of Computational and Applied Mathematics*, 211: 131–140, 2008.

[25] D. Izquierdo, C. Alonso, C. Andrade, and M. Castellote. Potentiostatic determination of chloride threshold values for rebar depassivation: experimental and statistical study. *Electrochim. Acta*, 49:2731–2739, 2004.

[26] R. Polder. Critical chloride content for reinforced concrete and its relationship to concrete resistivity. *Mater. Corros.*, 60: 623–630, 2009.

[27] R.E. Melchers. *Structural Reliability Analysis and Prediction*. John , Wiley & Sons, Chichester, second edition, 1999.

[28] P. Konečný. *Reliability of reinforced concrete bridge decks with respect to ingress of chlorides*. PhD thesis, VŠB Technical University Of Ostrava, Ostrava, Czech Republic, 2007.

[29] C. Andrade. Métodos modernos de cálculo de la vida útil del proyecto de estructuras de hormigón armado. *Hormigón*, pages 40–47, 1994. (Only available in Spanish).

[30] J. Crank. *The Mathematics of Diffusion*. Oxford Science Publications, 1975.

[31] H. Grube C. Andrade L.-O. Nilsson J. Kropp, H.K. Hilsdorf. Transport mechanisms and definitions. In J. Kropp and H. K. Hilsdorf, editors, *Performance Criteria for Concrete Durability*, pages 4–14, London, 1995. E & FN Spon.

[32] G. de Vera, M. A. Climent, E. Viqueira, C. Antón, and M. P. López. Chloride penetration prediction in concrete through an empirical model based on constant flux diffusion. *J. Mater. Civ. Eng.*, 27(8):04014231:1–9, 2015. doi: 10.1061/(ASCE) MT.1943-5533.0001173.

[33] J. Kropp. Chlorides in concrete. In J. Kropp and H. K. Hilsdorf, editors, *Performance Criteria for Concrete Durability*, pages 138–164, London, 1995. E & FN Spon.

[34] U. Angst, A. Rønnquist, B. Elsener, C. K. Larsen, and Ø. Vennesland. Probabilistic considerations on the effect of specimen size on the critical chloride content in reinforced concrete. *Corrosion Science*, 53:177–187, 2011.

[35] P. Sandberg, L. Tang, and A. Andersen. Recurrent studies of chloride ingress in uncracked marine concrete at various exposure times and elevations. *Cem Concr Res*, 28(10):1489–1503, 1998.

[36] CEN/TC 104. *Testing hardened concrete–determination of the chloride resistance of concrete, unidirectional diffusion.*

Final draft prCEN/TS 12390-11, 2013.

[37] A. Costa and J. Appleton. Chloride penetration into concrete in marine environment. Part I: Main parameters affecting chloride penetration. *Mater and Struct*, 32:252–259, 1999.

[38] M. D. A. Thomas and P. B. Bamforth. Modelling chloride diffusion in concrete. effect of fly ash and slag. *Cem Concr Res*, 29:487–495, 1999.

[39] L. Tang. Chloride ingress in concrete exposed to marine environment — Field data up to 10 years' exposure. Technical Report 16, SP Swedish National Testing and Research Institute, Borås, Sweden, 2003.

[40] K. Y. Ann, J. H. Ahn, and J. S. Ryou. The importance of chloride content at the concrete surface in assessing the time to corrosion of steel in concrete structures. *Const Build Mat*, 23:239–245, 2009.

[41] EN 1991. Eurocode 1: Basis of design and actions on structures. Technical report, CEN, 2000.